Supplementary Information

Synthesis of Caffeine Derivatives and Evaluation of Their Anticholinesterase Activities

Gabriela M. Furlani,[a] Júnio G. Silva,[b] Luana L. Dutra,[c] João P. V. Leite,[c] Felipe T. Martins,[d] Antonio J. Demuner,*[a] Eduardo V. V. Varejão[a] and Marcelo H. dos Santos[a]

[a]Departamento de Química, Universidade Federal de Viçosa, Campus Universitário, 36570-900 Viçosa-MG, Brazil

[b]Departamento de Química, Universidade Federal de Minas Gerais, Pampulha, 31270-901 Belo Horizonte-MG, Brazil

[c]Departamento de Bioquímica e Biologia Molecular, Universidade Federal de Viçosa, Campus Universitário, 36570-900 Viçosa-MG, Brazil

[d]Instituto de Química, Universidade Federal de Alfenas, Centro, 37130-001 Alfenas-MG, Brazil

---

*e-mail: ademuner@ufv.br

Gabriela M. Furlani: https://orcid.org/0000-0003-0369-5285
Júnio G. Silva: https://orcid.org/0000-0002-3714-3633
Luana L. Dutra: https://orcid.org/0000-0003-1553-1886
João P. V. Leite: https://orcid.org/0000-0002-3747-4424
Felipe T. Martins: https://orcid.org/0000-0001-9004-0927
Antonio J. Demuner: https://orcid.org/0000-0001-8918-2581
Eduardo V. V. Varejão: https://orcid.org/0000-0002-1830-725X
Marcelo H. Dos Santos: https://orcid.org/0000-0003-1440-4340

Compound characterization spectra

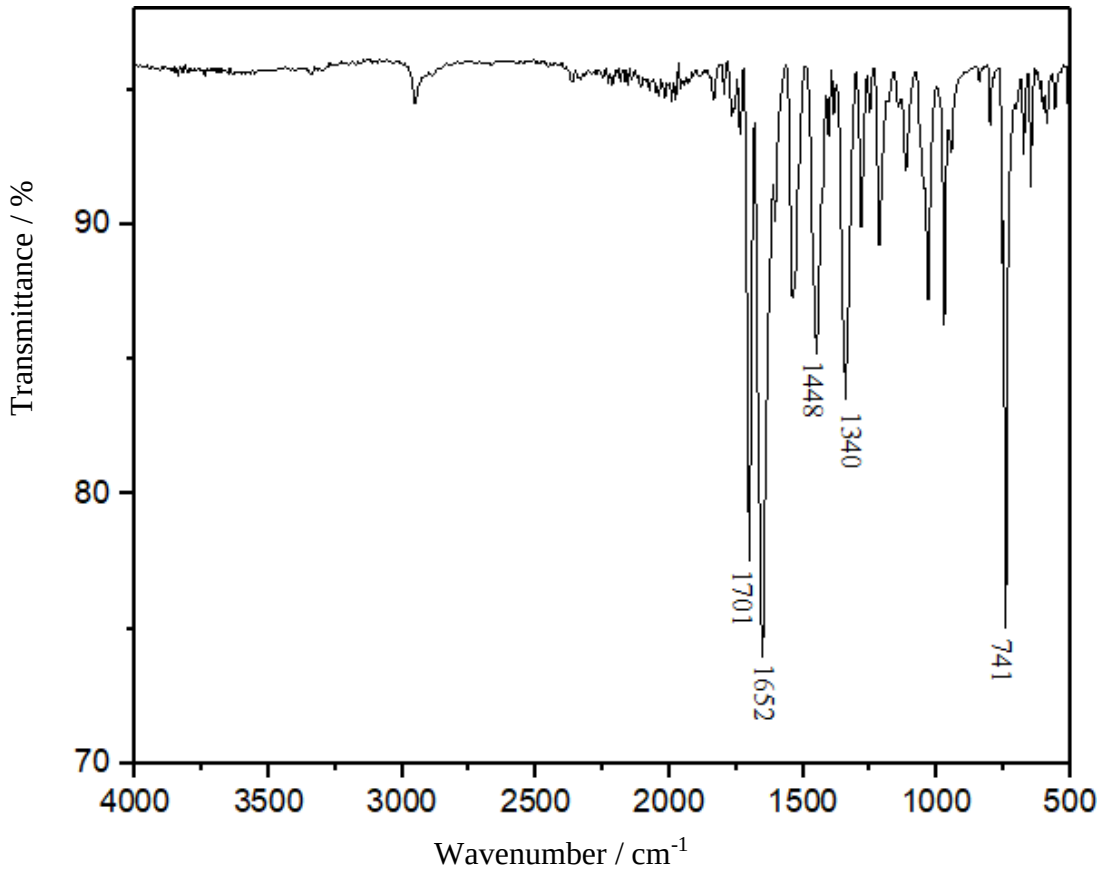

Figure S1. ATR-FTIR spectrum of the CAF-Br (**2**) compound.

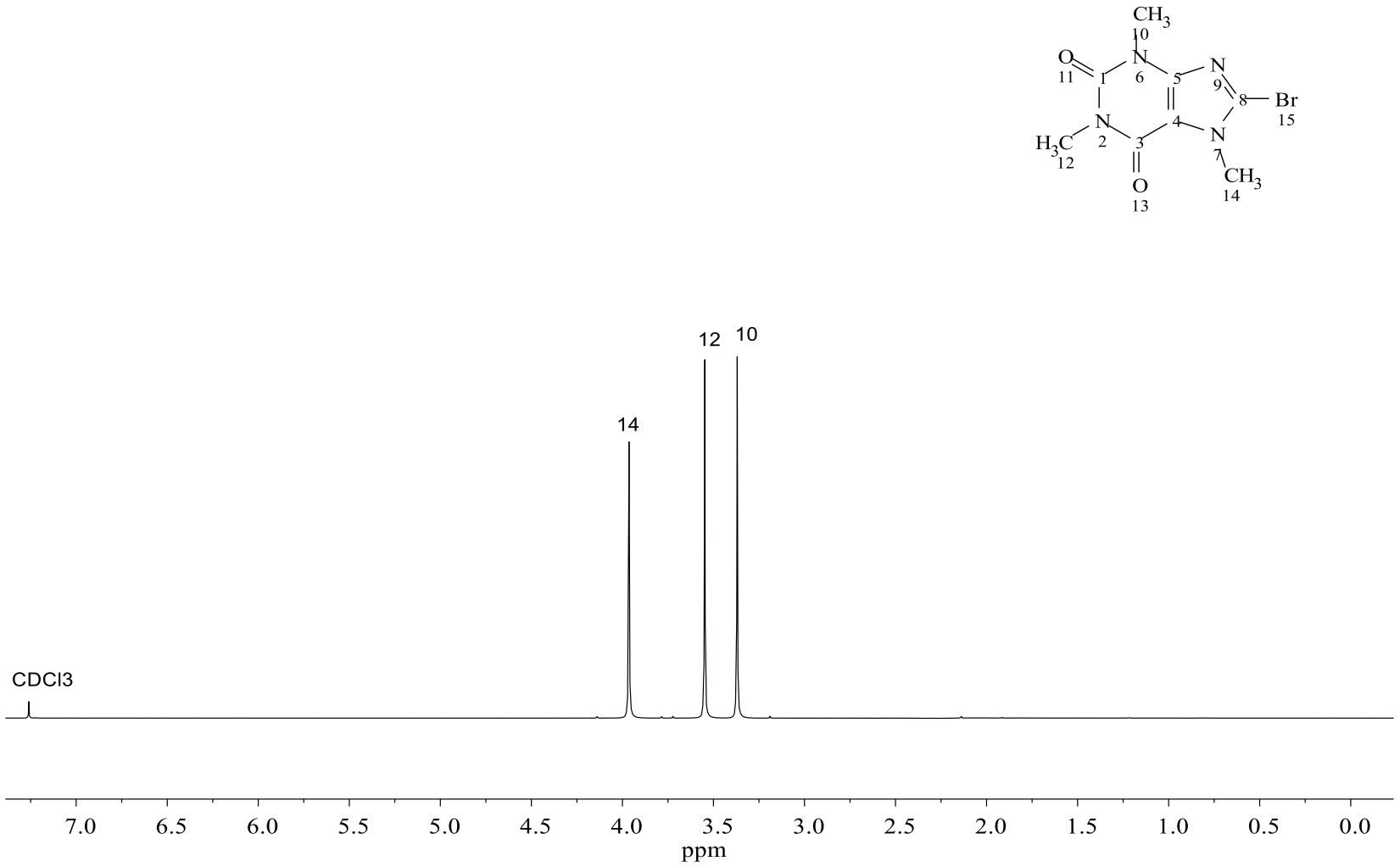

Figure S2. ^{1}H NMR spectrum (400 MHz, $CDCl_3$) of the CAF-Br (**2**) compound.

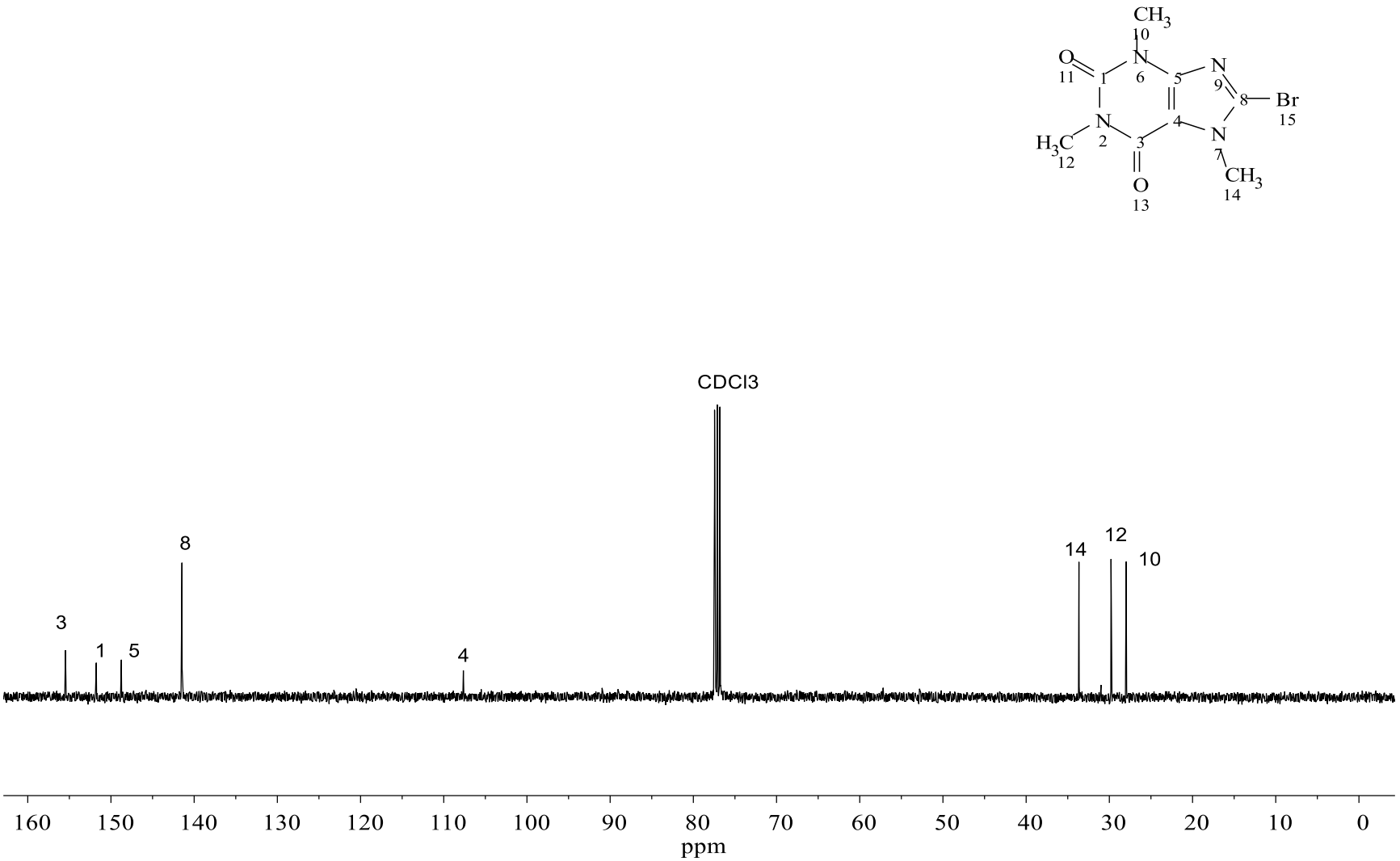

Figure S3. ^{13}C NMR spectrum (100 MHz, $CDCl_3$) of the CAF-Br (**2**) compound.

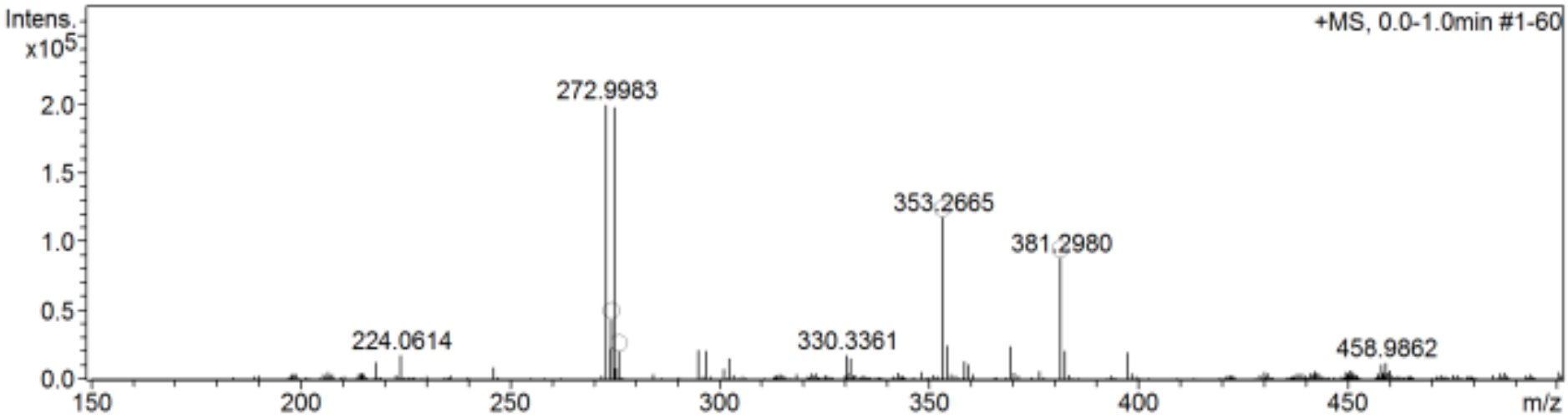

Figure S4. ESI-(+)-MS spectrum (50-1000 *m/z*) of the CAF-Br (**2**) compound.

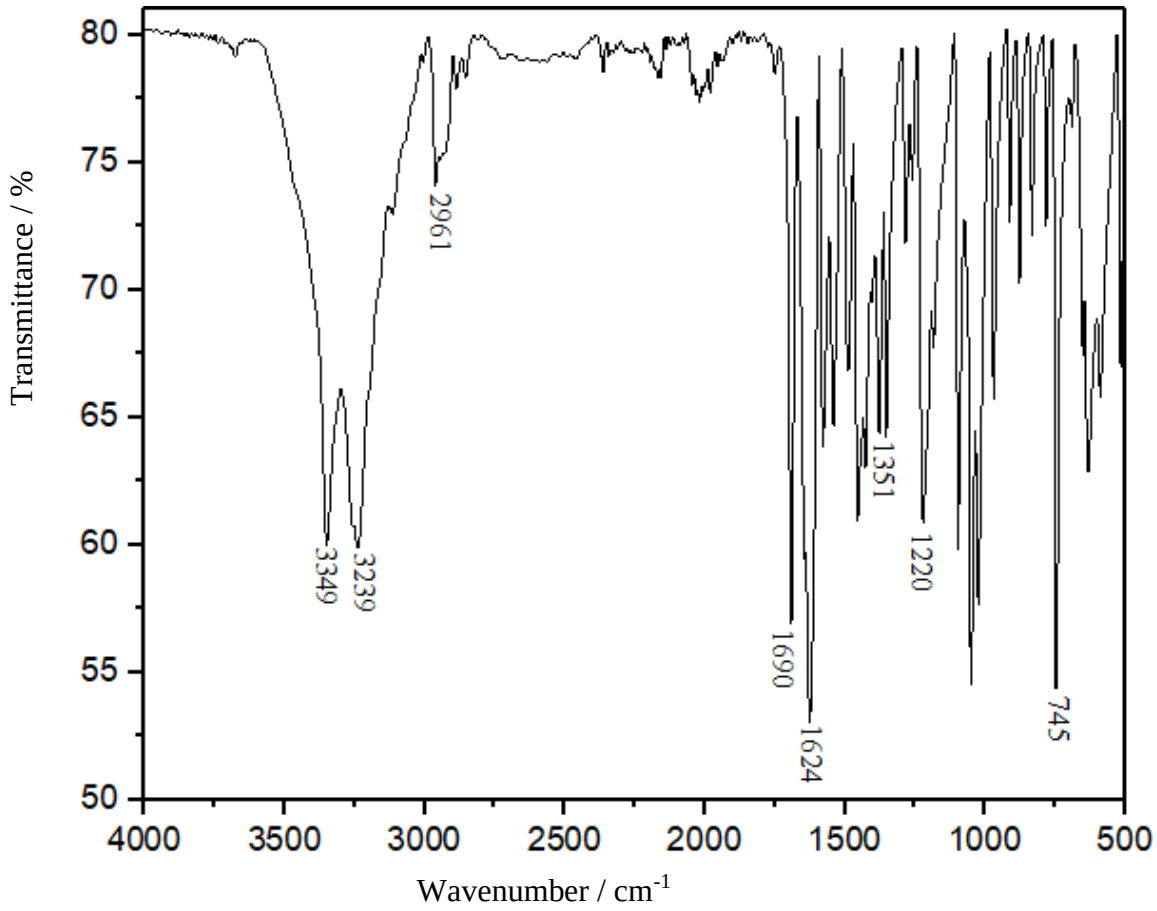

Figure S5. ATR-FTIR spectrum of the CAF-Ethanolamine (**3**) compound.

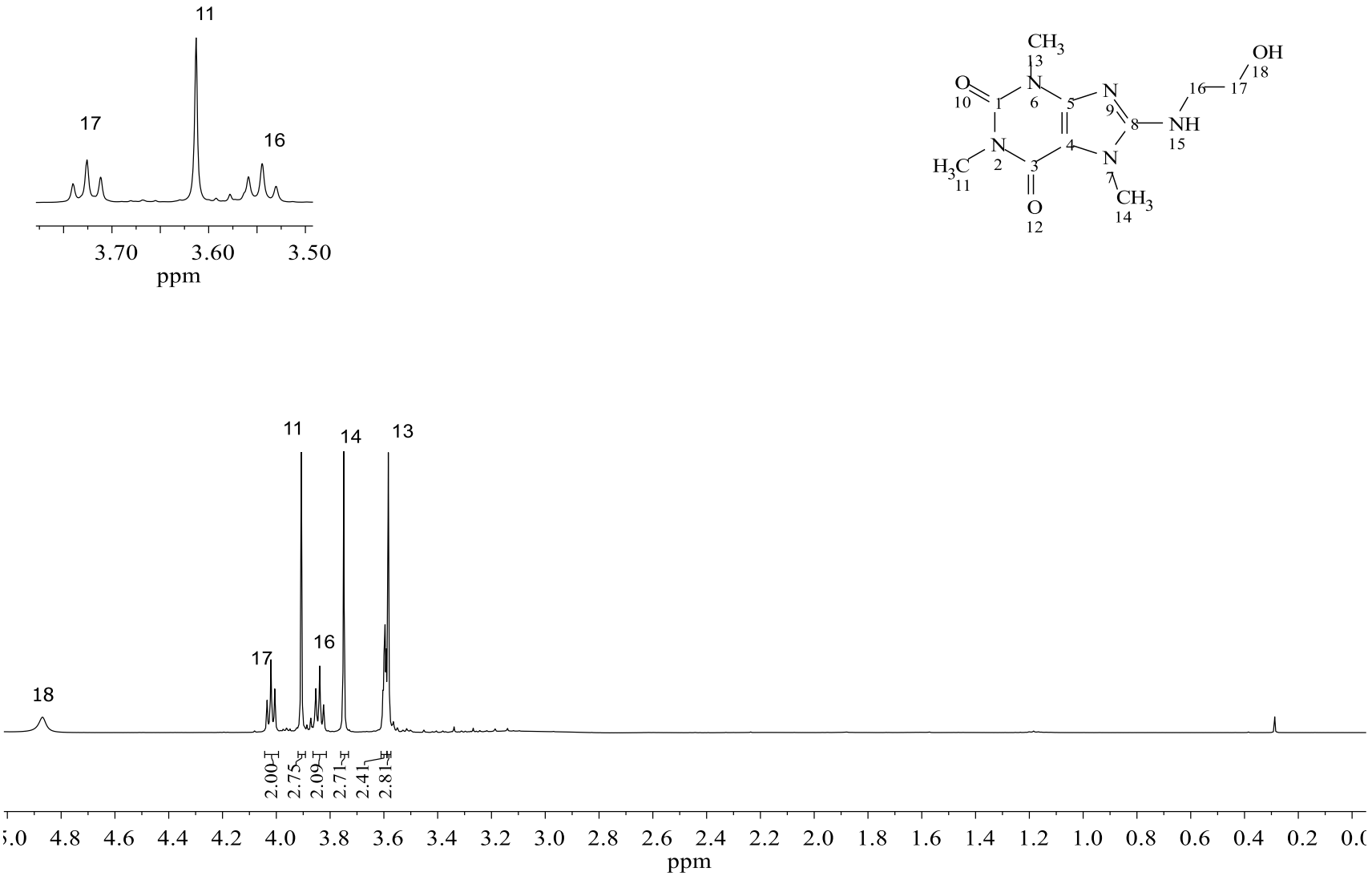

Figure S6. ^{1}H NMR spectrum (400 MHz, MeOD) of the CAF-Ethanolamine (**3**) compound.

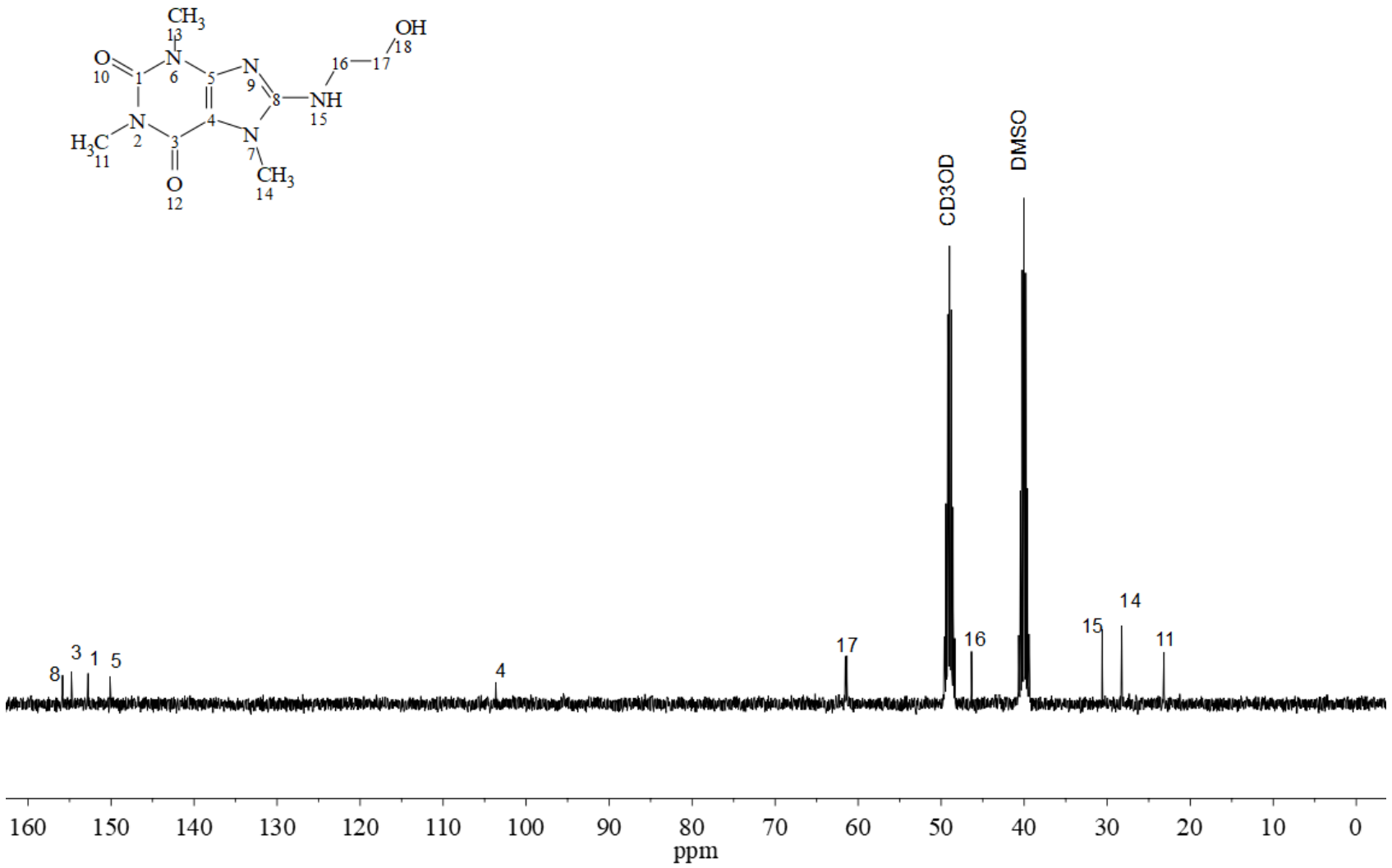

Figure S7. ^{13}C NMR spectrum (100 MHz, MeOD) of the CAF-Ethanolamine (**3**) compound.

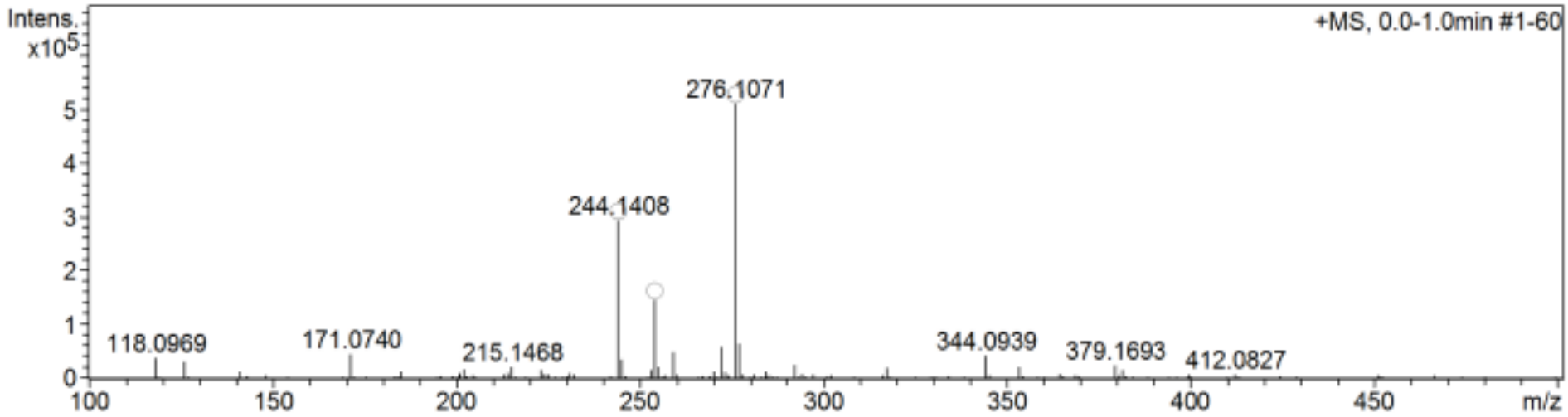

Figure S8. ESI-(+)-MS spectrum (50-1000 *m/z*) of the CAF-Ethanolamine (**3**) compound.

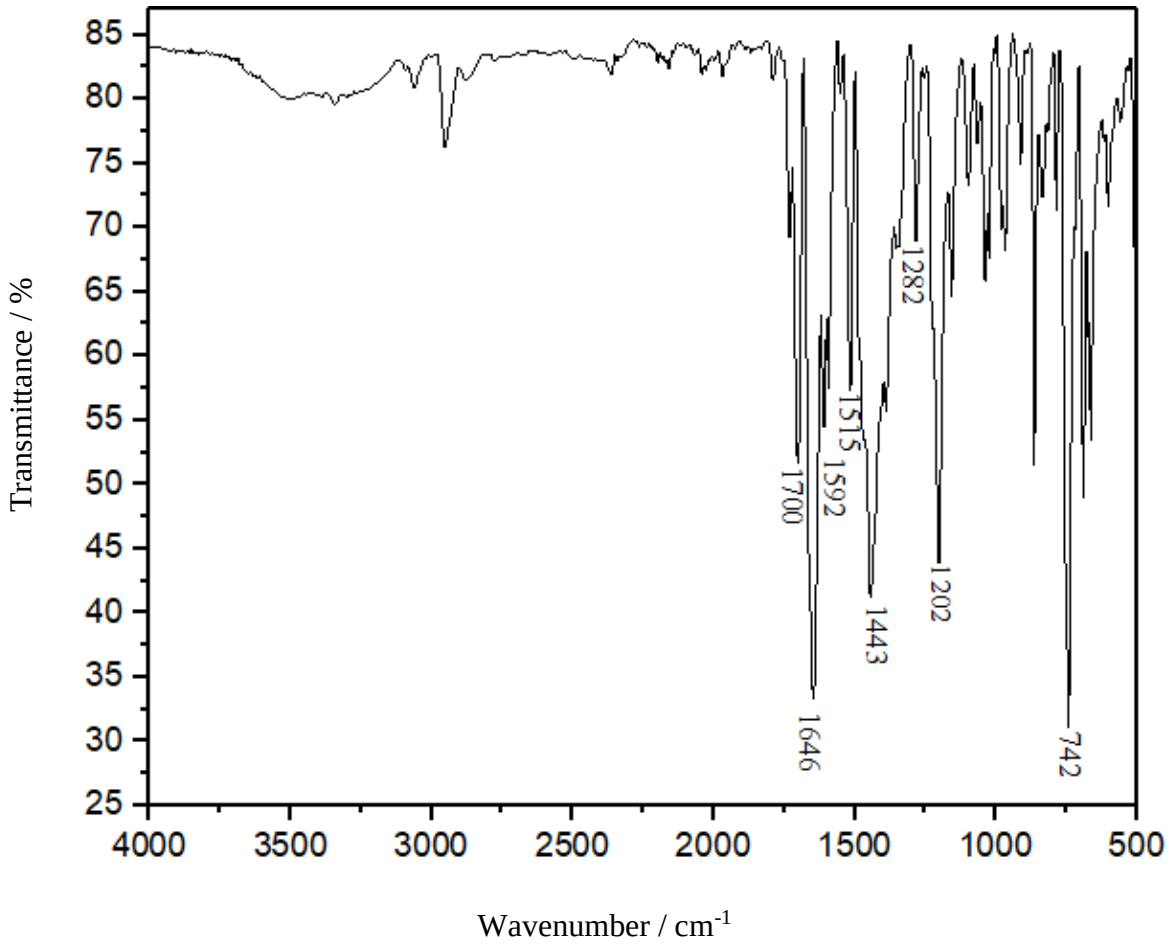

Figure S9. ATR-FTIR spectrum of the CAF-Phenol (**4**) compound.

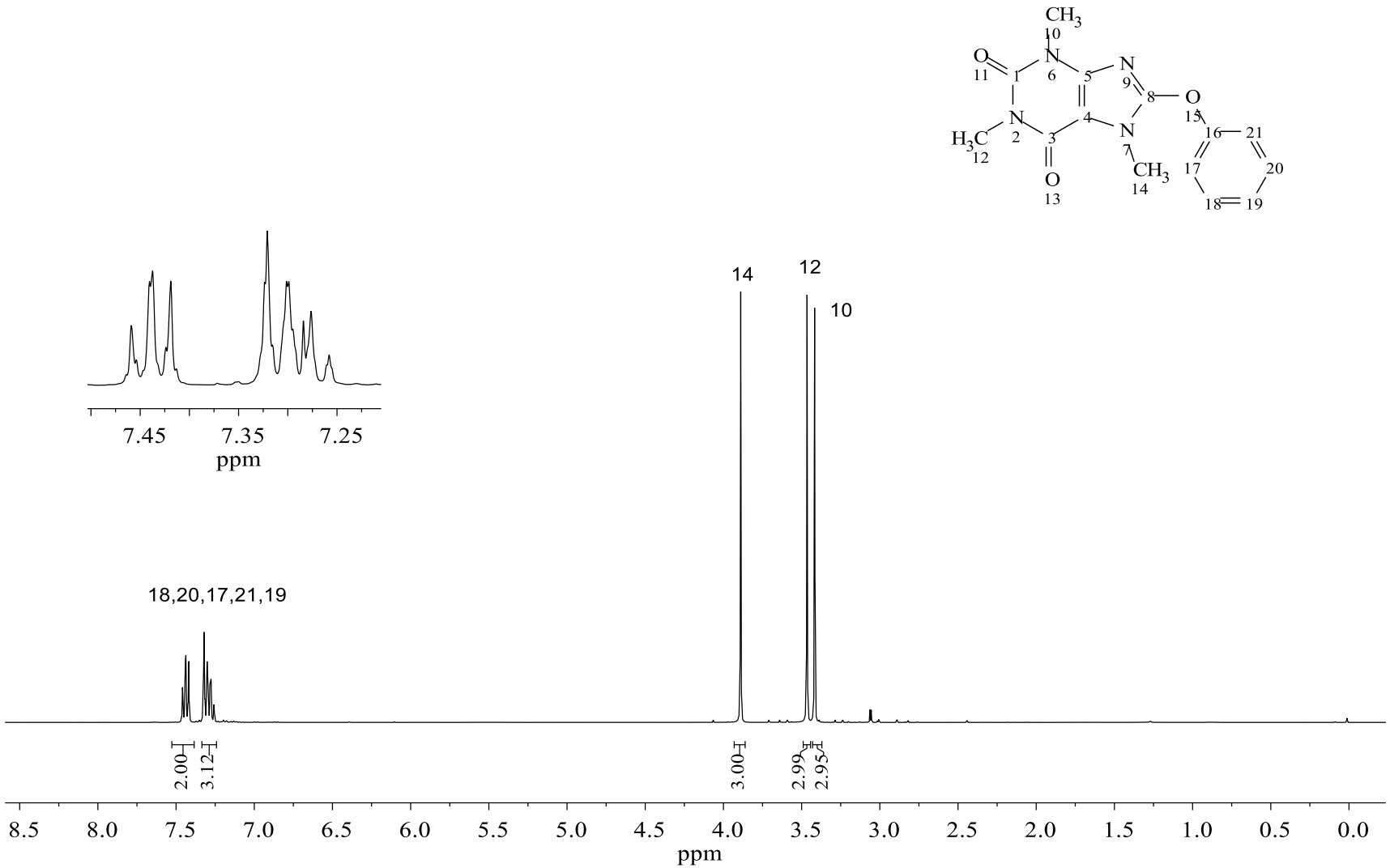

Figure S10. ^{1}H NMR spectrum (400 MHz, $CDCl_3$) of the CAF-Phenol (**4**) compound.

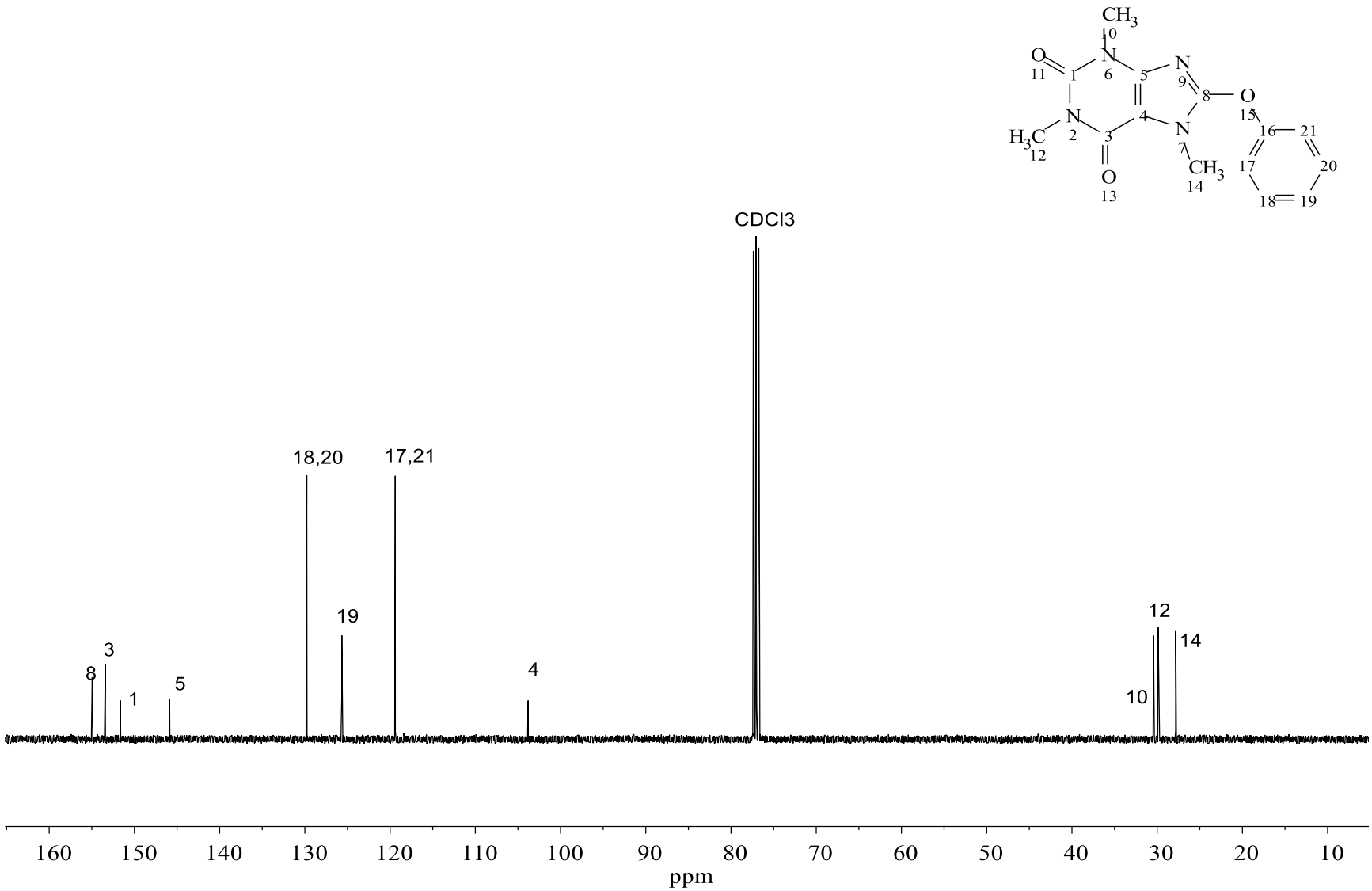

Figure S11. ^{13}C NMR spectrum (100 MHz, $CDCl_3$) of the CAF-Phenol (**4**) compound.

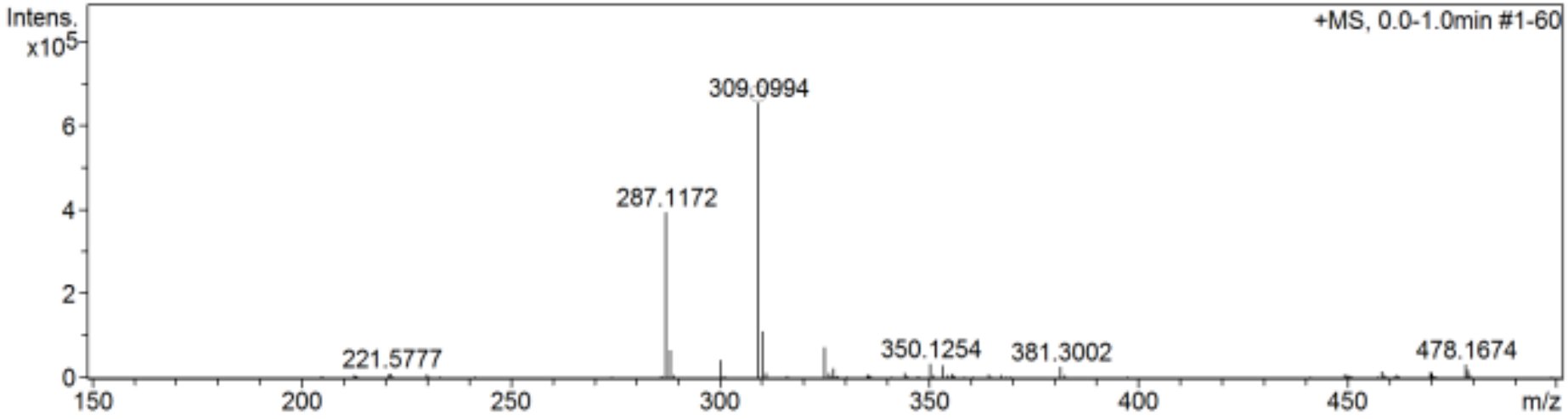

Figure S12. ESI-(+)-MS spectrum (50-1000 *m/z*) of the CAF-Phenol (**4**) compound.

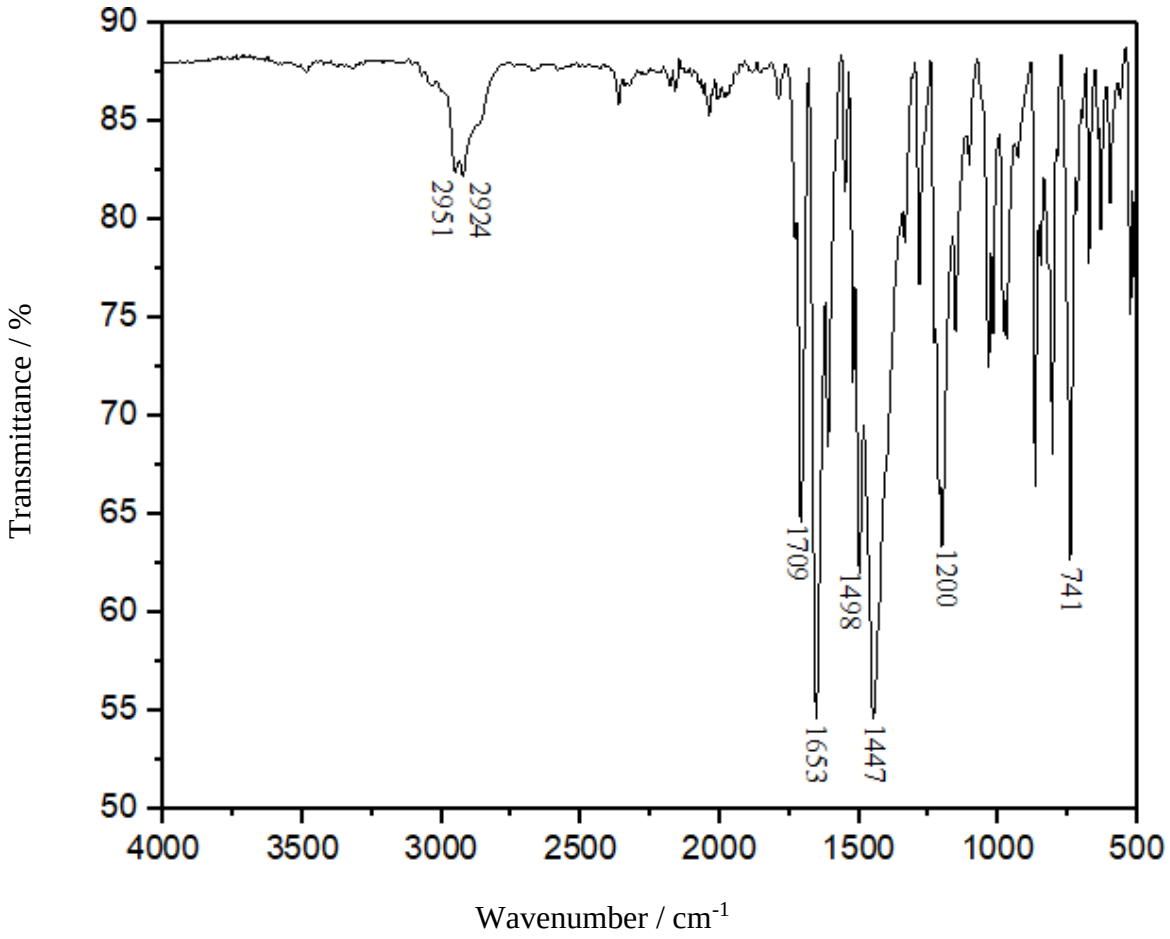

Figure S13. ATR-FTIR spectrum of the CAF-*p*-Cresol (**5**) compound.

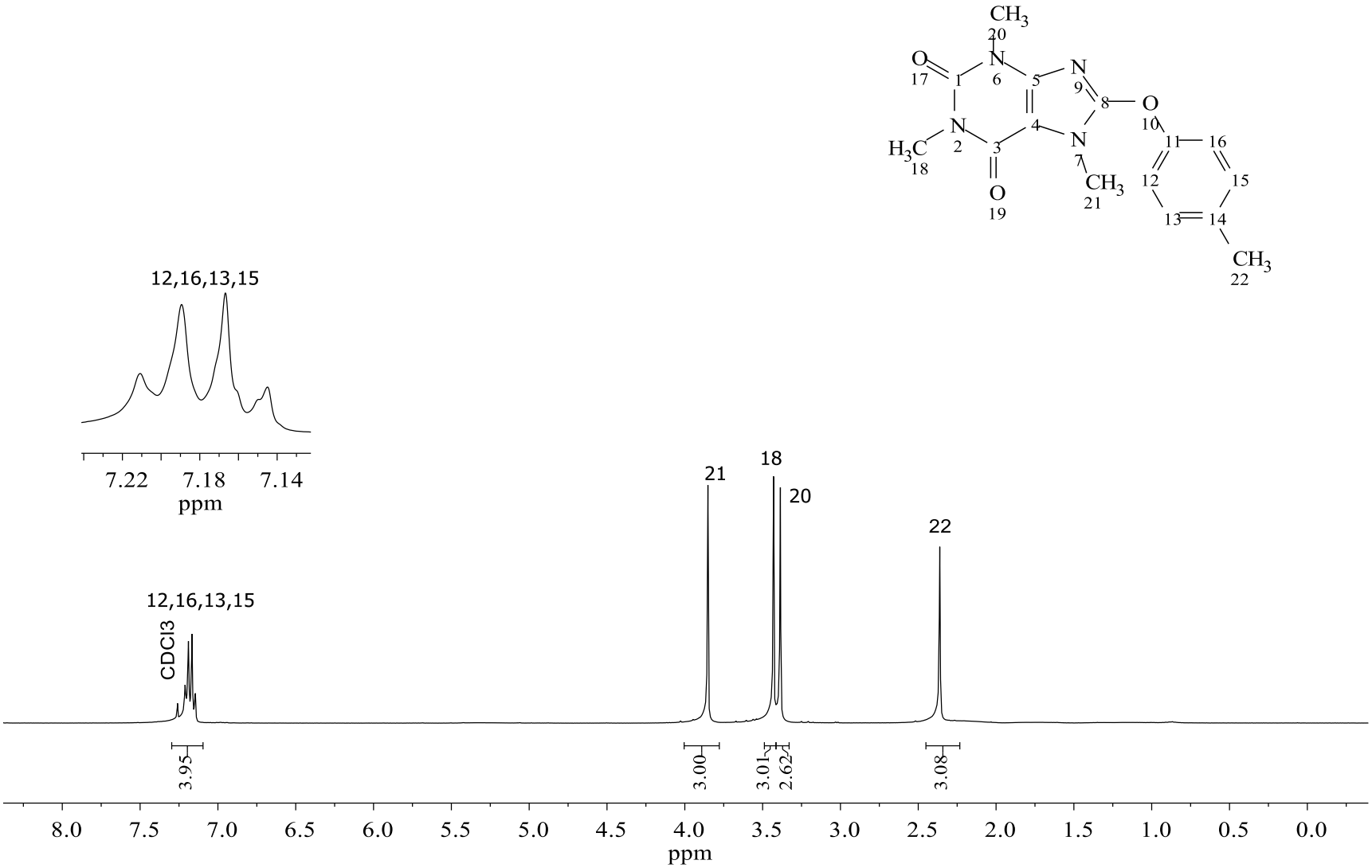

Figure S14. ^{1}H NMR spectrum (400 MHz, $CDCl_3$) of the CAF-*p*-Cresol (**5**) compound.

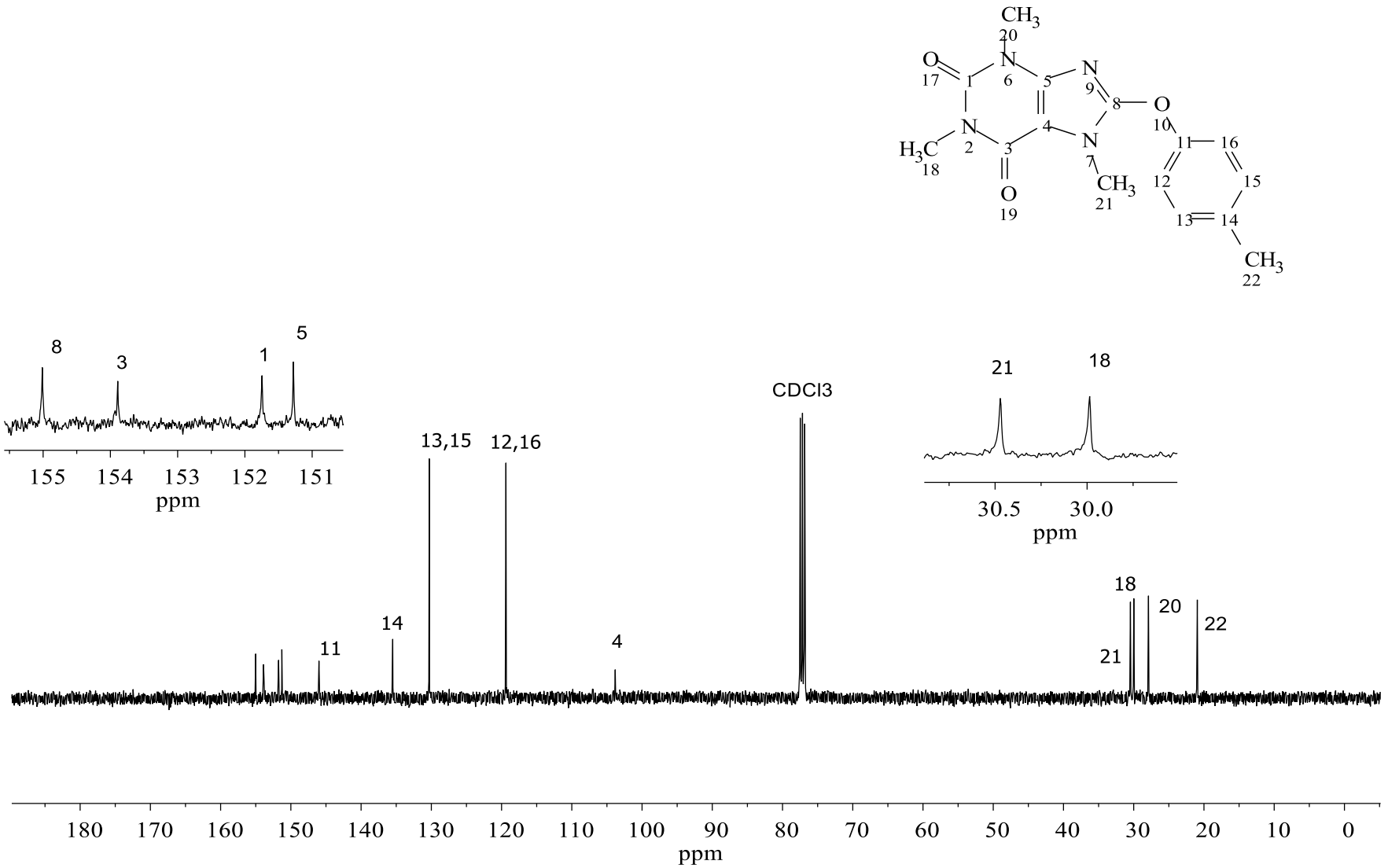

Figure S15. ^{13}C NMR spectrum (100 MHz, $CDCl_3$) of the CAF-*p*-Cresol (**5**) compound.

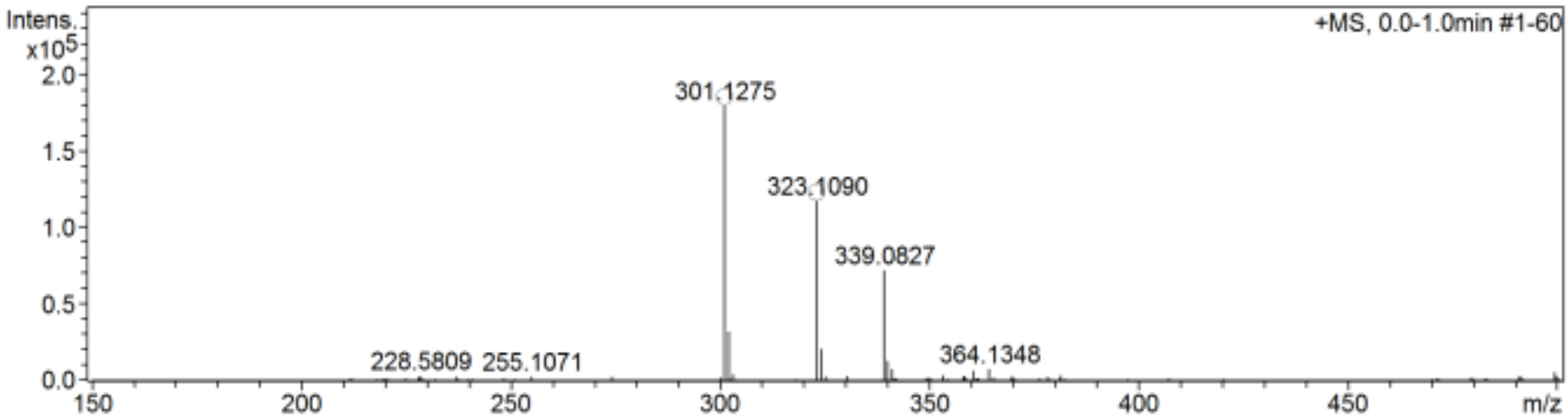

Figure S16. ESI-(+)-MS spectrum (50-1000 *m/z*) of the CAF-*p*-Cresol (**5**) compound.

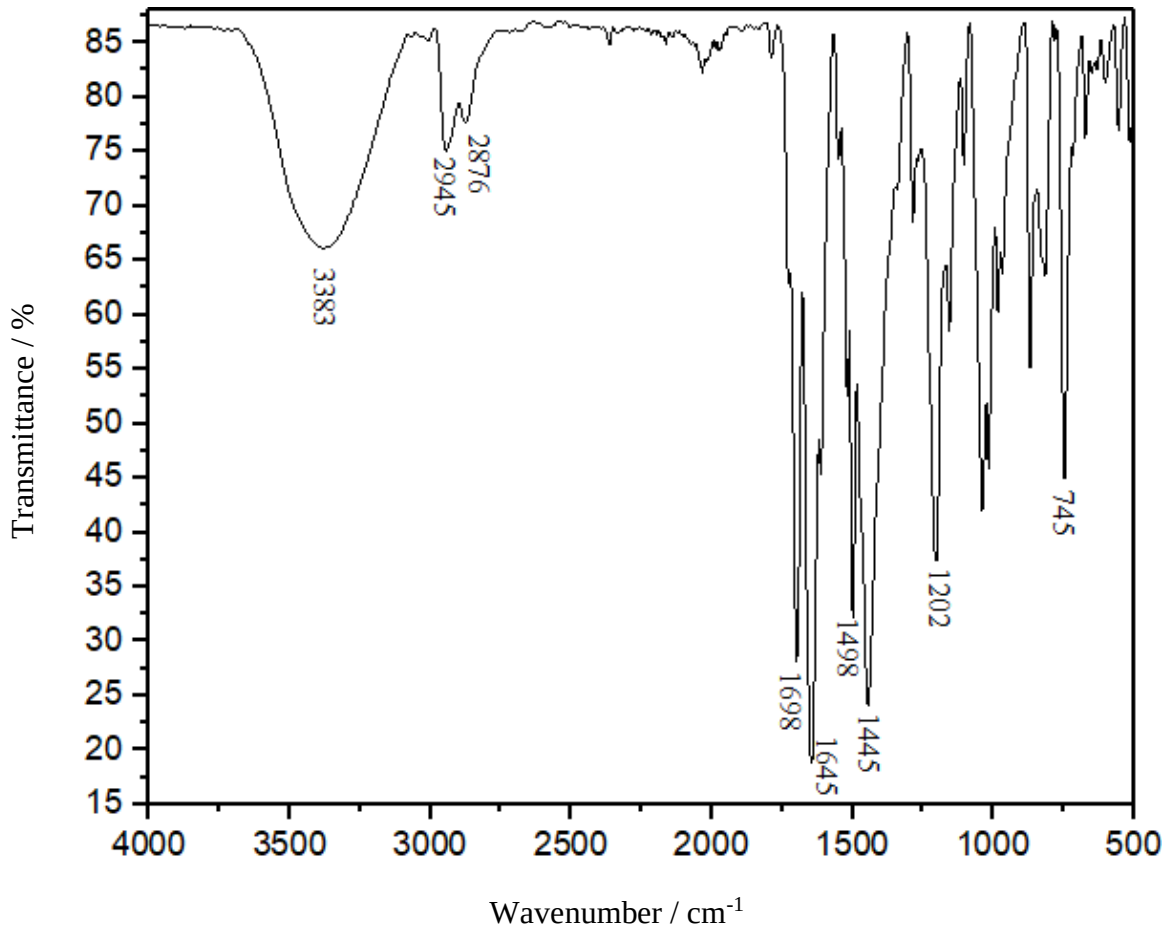

Figure S17. ATR-FTIR spectrum of the CAF-Tyrosol (**6**) compound.

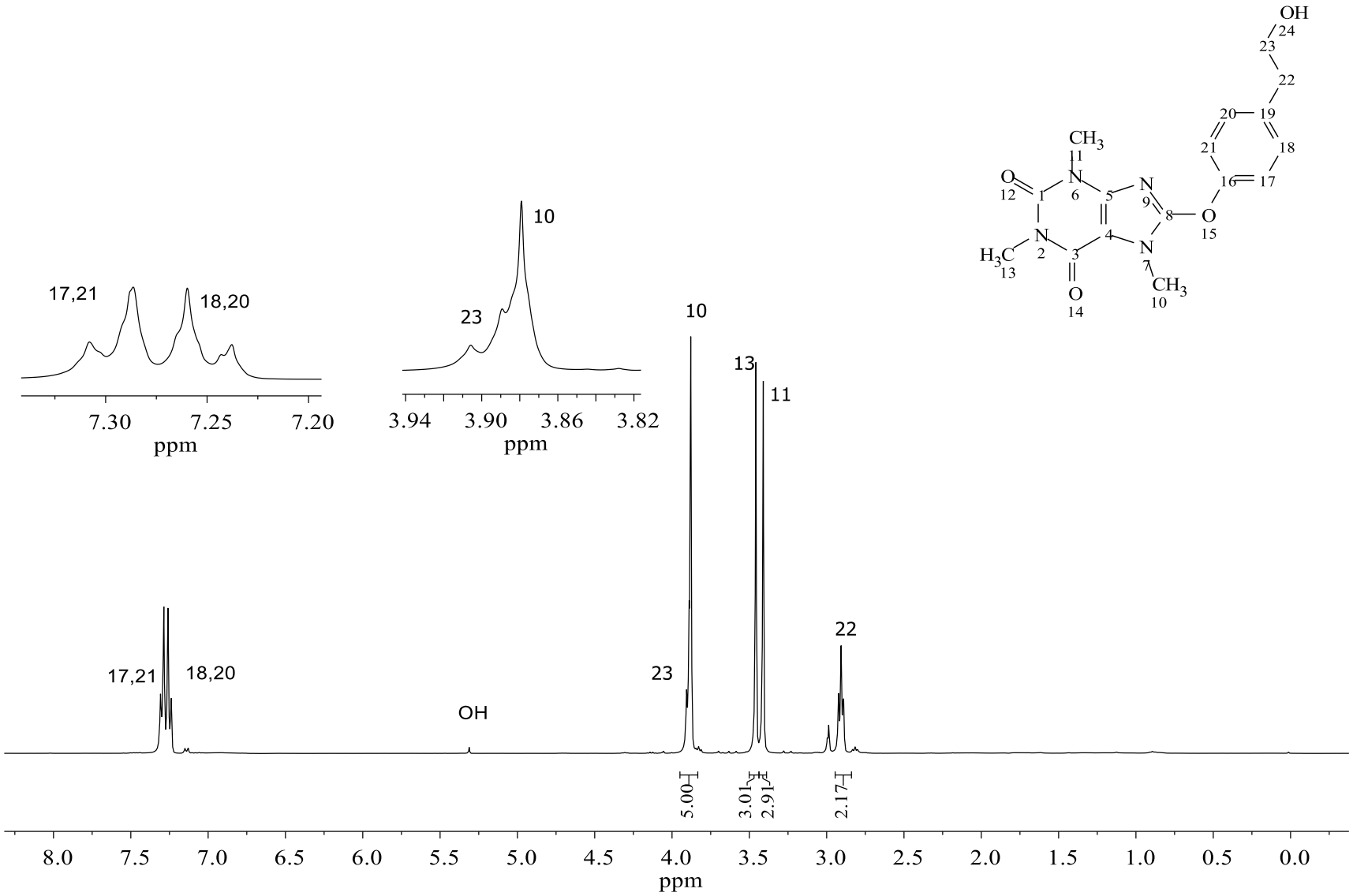

Figure S18. ^{1}H NMR spectrum (400 MHz, $CDCl_3$) of the CAF-Tyrosol (**6**) compound.

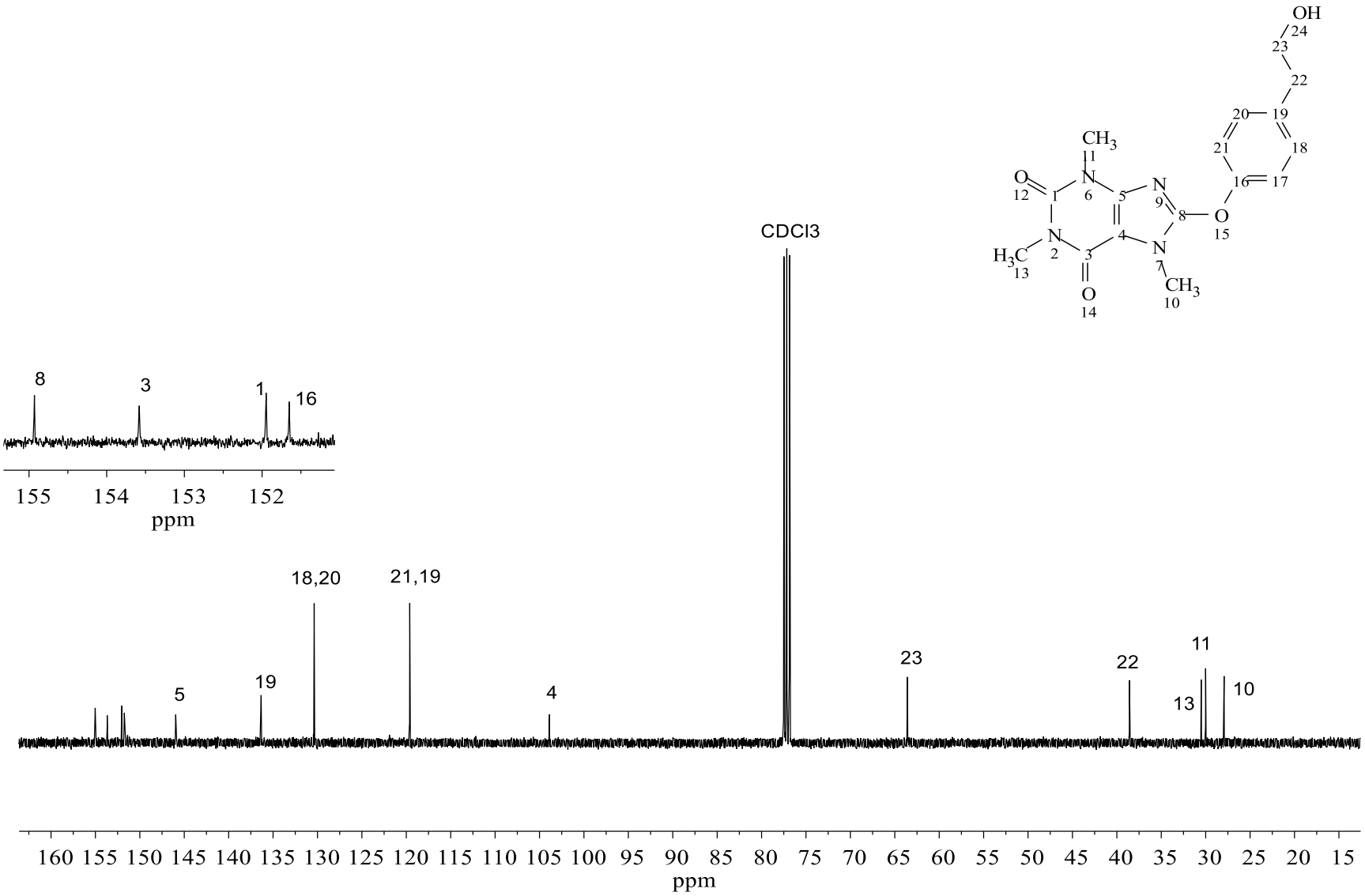

Figure S19. ^{13}C NMR spectrum (100 MHz, $CDCl_3$) of the CAF-Tyrosol (**6**) compound.

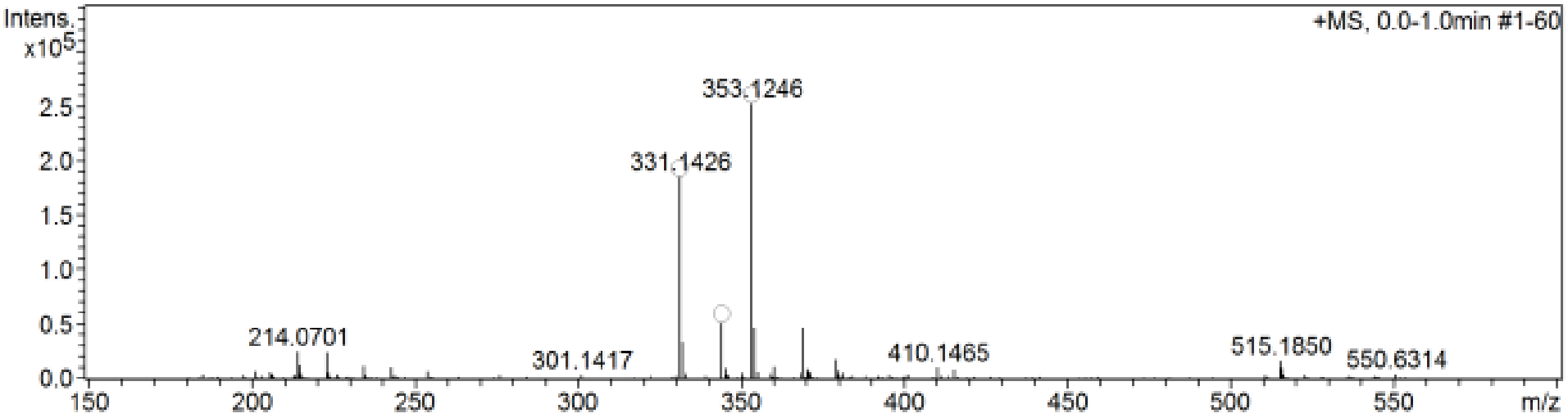

Figure S20. ESI-(+)-MS spectrum (50*1000 *m/z*) of the CAF-Tyrosol (**6**) compound.

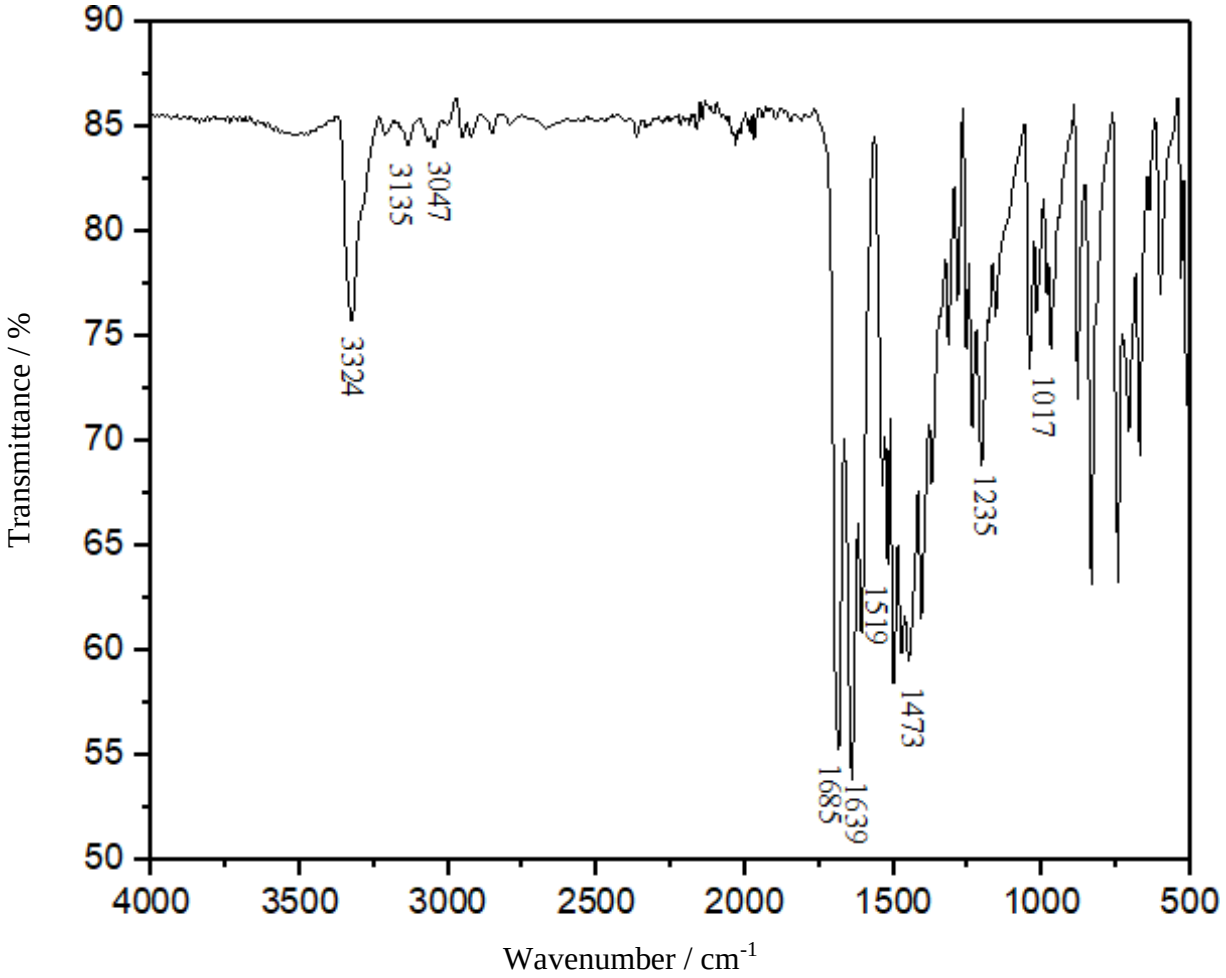

Figure S21. ATR-FTIR spectrum of the CAF-Paracetamol (**7**) compound.

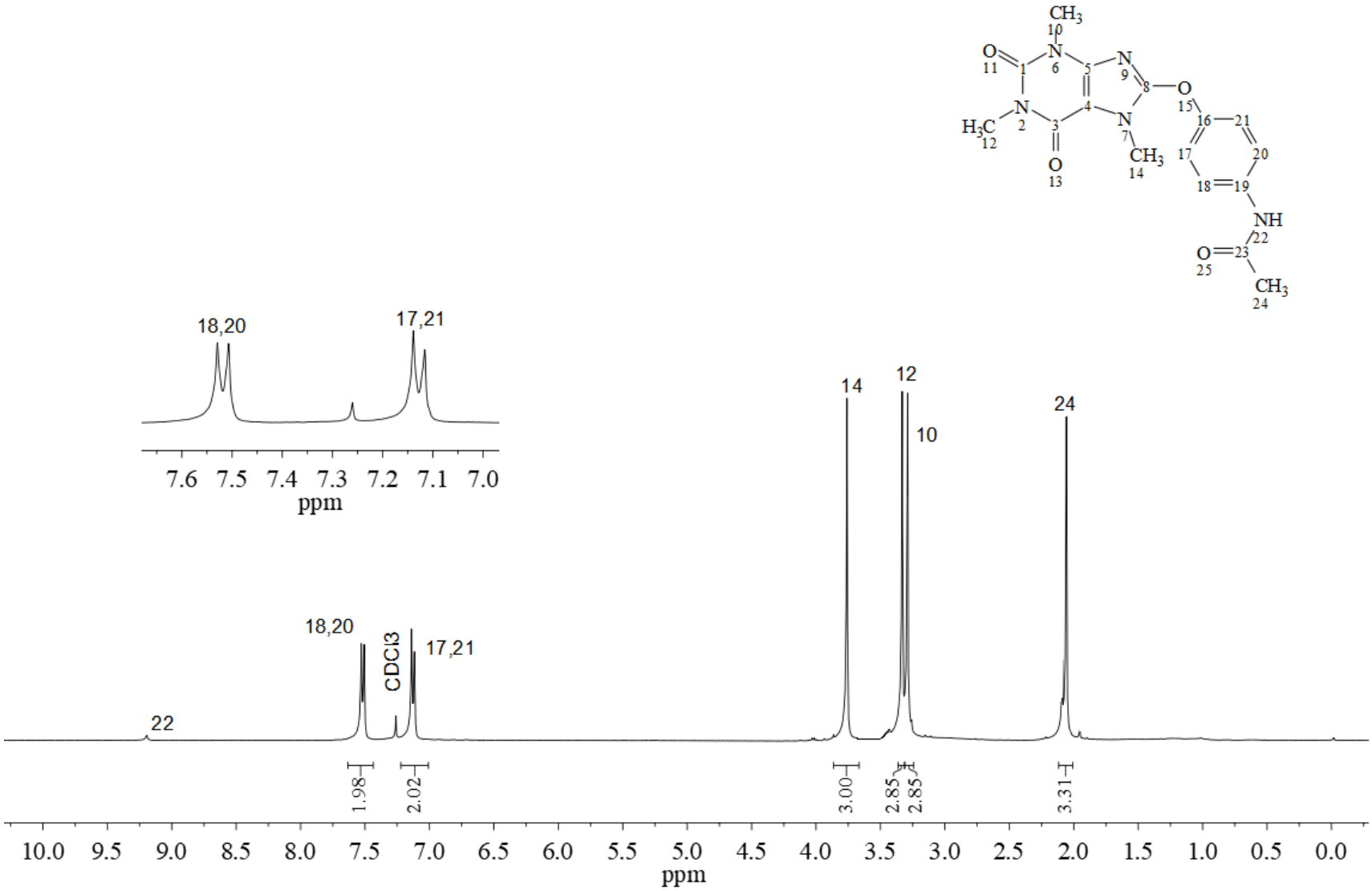

Figure S22. ^{1}H NMR spectrum (400 MHz, $CDCl_3$) of the CAF-Paracetamol (**7**) compound.

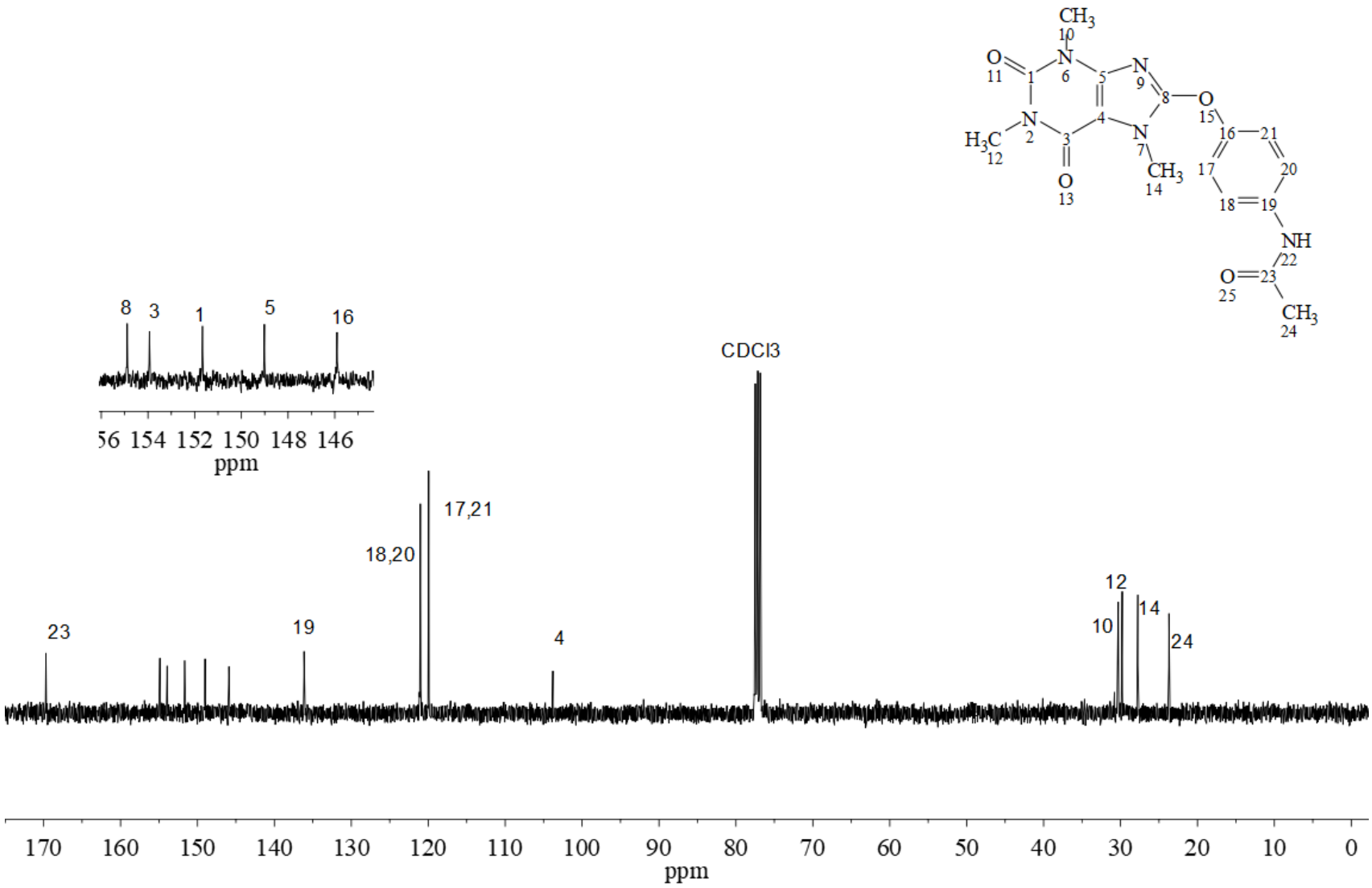

Figure S23. ^{13}C NMR spectrum (100 MHz, $CDCl_3$) of the CAF-Paracetamol (**7**) compound.

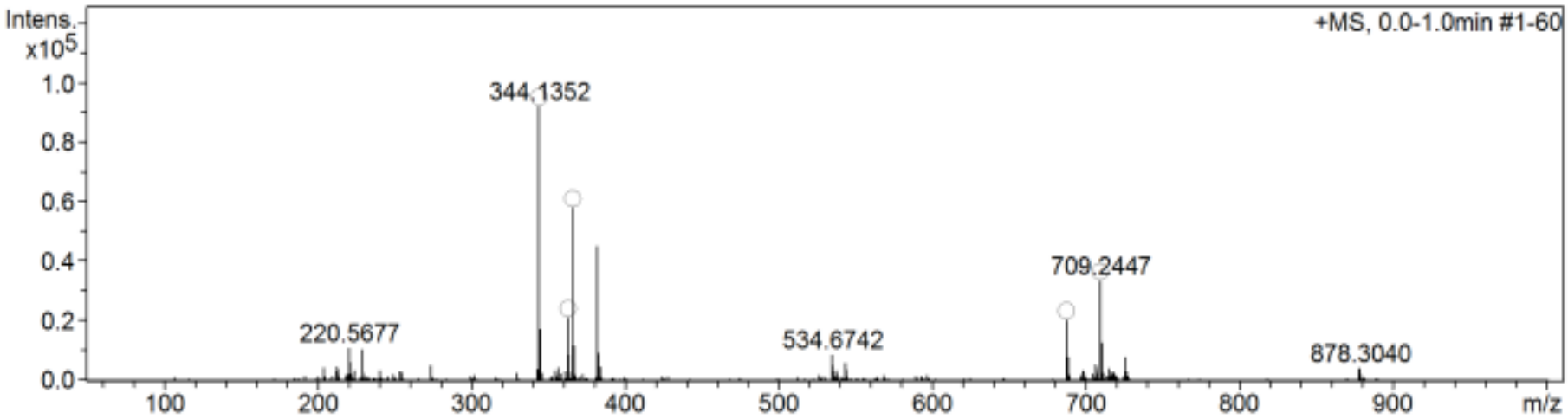

Figure S24. ESI-(+)-MS spectrum (50-1000 *m/z*) of the CAF-Paracetamol (**7**) compound.

Atomic coordinates of the stationary points and spin density maps calculated by DFT

Intermediate **1**

	Atom		Cartesian Coordinates (Angstroms) X	Y	Z
1	C	C1	-0.1577283	-1.3625064	0.0000000
2	C	C2	-0.3734526	1.0835187	0.0000000
3	C	C3	1.8308119	0.1578268	0.0000000
4	N	N1	0.9891717	1.2729347	0.0000000
5	N	N2	1.2193757	-1.1149847	0.0000000
6	C	C4	-0.9167882	-0.1686025	0.0000000
7	N	N3	-2.2545956	0.0965644	0.0000000
8	C	C5	-2.5170748	1.4033049	0.0000000
9	N	N4	-1.3481375	2.0494623	0.0000000
10	O	O1	-0.6671559	-2.4781599	0.0000000
11	O	O2	3.0597455	0.2728275	0.0000000
12	C	C6	2.1156485	-2.2551186	0.0000000
13	C	C7	1.5414126	2.6155569	0.0000000
14	C	C8	-3.3173638	-0.8786896	0.0000000
15	H	H1	2.7543019	-2.2051900	0.8880391
16	H	H2	2.7543019	-2.2051900	-0.8880391
17	H	H3	1.5828837	-3.2091865	0.0000000
18	H	H4	1.1950116	3.1433610	0.8941720
19	H	H5	1.1950116	3.1433610	-0.8941720
20	H	H6	2.6344293	2.6080709	0.0000000
21	H	H7	-3.2276919	-1.4899060	0.9007445
22	H	H8	-3.2276919	-1.4899060	-0.9007445
23	H	H9	-4.2747647	-0.3523337	0.0000000

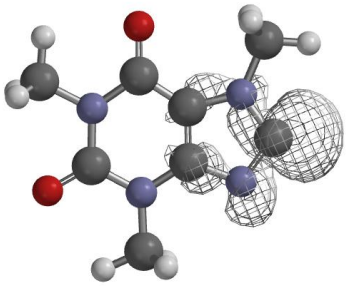

spin density map

Intermediate **2**

	Atom		Cartesian Coordinates (Angstroms) X	Y	Z
1	C	C1	-0.1472385	-1.3938254	-0.0124927
2	C	C2	-0.2870862	1.0539338	0.0023916
3	C	C3	1.9029953	0.0755780	-0.0135279
4	N	N1	1.0769464	1.2081810	-0.0009411
5	N	N2	1.2560453	-1.2011564	-0.0200535
6	C	C4	-0.8771761	-0.1723771	-0.0031034
7	N	N3	-2.2197934	0.0815300	0.0017022
8	C	C5	-2.3698541	1.4428568	0.0116765
9	N	N4	-1.2043162	2.0585642	0.0131481
10	C	C6	2.0924125	-2.3820405	-0.0641328
11	C	C7	1.6552348	2.5412078	0.0045569
12	O	O1	3.1352016	0.1880800	-0.0119343
13	O	O2	-0.7090561	-2.4882926	-0.0068169
14	C	C8	-3.2842958	-0.8904876	-0.0044486
15	H	H1	-3.3376826	1.9292073	0.0172959
16	H	H2	1.5956743	-3.2829072	0.3315376
17	H	H3	3.1113789	-2.2057993	0.3185740
18	H	H4	1.3223702	3.0709379	0.9028180
19	H	H5	1.3170620	3.0805395	-0.8859828
20	H	H6	2.7478807	2.5143223	0.0010865
21	H	H7	-4.2482270	-0.3751262	-0.0035796
22	H	H8	-3.1935751	-1.5000852	-0.9068682
23	H	H9	-3.1961715	-1.5082960	0.8926213

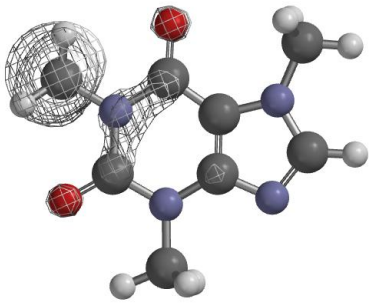

spin density map

Intermediate **3**

	Atom		Cartesian Coordinates (Angstroms) X	Y	Z
1	C	C1	-0.0291063	-1.3371296	0.0030370
2	C	C2	-0.3934477	1.0925120	-0.0144169
3	C	C3	1.8780350	0.2899576	-0.0110949
4	N	N1	0.9647715	1.3701514	-0.0191648
5	N	N2	1.3307589	-1.0170397	-0.0047394
6	C	C4	-0.8671519	-0.1886116	-0.0025798
7	N	N3	-2.2288530	-0.0684073	0.0004676
8	C	C5	-2.5169423	1.2695001	-0.0050221
9	N	N4	-1.4212795	2.0002593	-0.0109389
10	O	O1	-0.4724124	-2.4805433	0.0163476
11	O	O2	3.1045658	0.4548584	-0.0036676
12	C	C6	2.2883317	-2.1069964	0.0004512
13	C	C7	1.4106558	2.7239685	-0.0651016
14	C	C8	-3.1907244	-1.1423057	0.0075649
15	H	H1	-3.5290179	1.6555666	-0.0042654
16	H	H2	2.9080665	-2.0300076	0.8998840
17	H	H3	2.9379514	-2.0155163	-0.8762668
18	H	H4	1.8087096	-3.0887227	-0.0160980
19	H	H5	0.6675561	3.4428893	0.3157999
20	H	H6	2.4360215	2.8552841	0.3152080
21	H	H7	-4.2015281	-0.7262938	0.0049106
22	H	H8	-3.0404697	-1.7498339	-0.8882878
23	H	H9	-3.0402010	-1.7380039	0.9112777

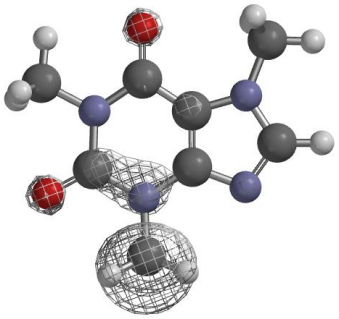

spin density map

Intermediate **4**

	Atom		Cartesian Coordinates (Angstroms) X	Y	Z
1	C	C1	-0.0560626	-1.3934320	-0.0033206
2	C	C2	-0.4615272	1.0188528	-0.0104945
3	C	C3	1.8101332	0.2728364	-0.0009647
4	N	N1	0.8811810	1.3139552	-0.0007753
5	N	N2	1.2993239	-1.0405436	-0.0430261
6	C	C4	-0.9180674	-0.2680028	-0.0121023
7	N	N3	-2.2692062	-0.1400136	-0.0167580
8	C	C5	-2.5684319	1.1946324	-0.0248087
9	N	N4	-1.4749039	1.9331608	-0.0110419
10	O	O1	-0.4529949	-2.5534582	0.0518881
11	O	O2	3.0254446	0.4834500	0.0392662
12	C	C6	2.2778744	-2.1117158	-0.0401098
13	C	C7	1.3241712	2.6969555	0.0254163
14	C	C8	-3.2251647	-1.1608529	-0.0685581
15	H	H1	-3.5839044	1.5655128	-0.0456703
16	H	H2	2.7314872	-2.1633340	0.9549556
17	H	H3	3.0646014	-1.8977424	-0.7708121
18	H	H4	1.8328523	-3.0808267	-0.2800111
19	H	H5	0.9616704	3.1692432	0.9439284
20	H	H6	0.9140612	3.2212066	-0.8436081
21	H	H7	2.4139774	2.7771305	-0.0022765
22	H	H8	-4.2079859	-0.8622900	0.3233540
23	H	H9	-2.8586696	-2.1303876	0.3017690

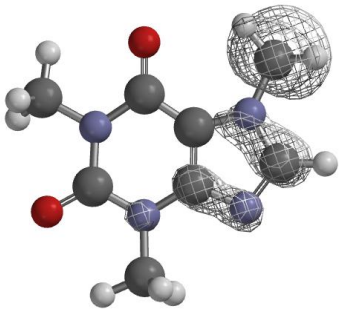

spin density map

Homology assessment between human AChE and the enzyme used in *in vitro* assays

Given that the evaluation of the cholinesterase potential of the compounds was conducted using AChE from *Torpedo californica*, it is necessary to perform a homology analysis between the enzyme employed in the assay and the enzyme from *Homo sapiens*. This analysis aims to ensure that the results obtained with the fish-derived enzyme are reproducible with the human enzyme. The homology result for this enzyme is presented in Figure S25.

The alignment between the human and fish AChE sequences revealed a significant degree of similarity. The root-mean-square deviation (RMSD) value obtained in this study was 0.63 Å. According to data reported in the literature,[1-4] RMSD values below 1.0 Å are considered acceptable to ensure a good level of homology between the evaluated enzymes.

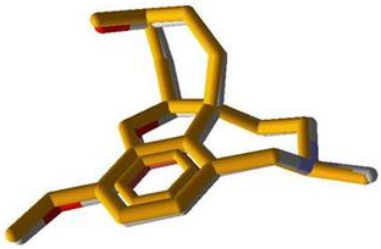

Figure S25. Re-docking of galantamine into human AChE (PDB ID: 4EY6). Galantamine co-crystallized with the enzyme is shown in element-based colors, while the galantamine pose obtained from the molecular docking study is shown in yellow.

Single crystal X-ray diffraction

Room temperature (296(2) K) single-crystal X-ray diffraction data were measured on a Bruker-AXS Kappa Duo X-ray diffractometer adapted with a Photon II CMOS detector. X-ray MoKα beam was generated from a microfocus source. Cell indexing and intensity dataset collect strategy setup and treatment were performed with the Bruker software SAINT and SADABS (Bruker AXS Inc., 2015). Structure solutions and refinements were dealt with SHELXS and SHELXL,[5] respectively. MERCURY (Cambridge Crystallographic Data Centre (CCDC), version 4.0)[6] was chosen to prepare the crystal structure projections. Non-hydrogen and hydrogen atoms were treated as anisotropic and isotropic ($1.2U_{iso}$(C or N) or $1.5U_{iso}$(C_{methyl} or O)) in the refinements, respectively. For hydrogen sites, a riding model was employed, with fixed bond lengths and angles following their bonded carbon, nitrogen or oxygen atoms. The entire X-ray diffraction datasets, loading all structure factors and RES refinement file, were deposited in CCDC under deposit code shown in Table S1. In this table, a summary of the crystal data collects, raw data treatments and the refinement statistical parameters can be found.

Table S1. Crystal data and refinement statistics for the two caffeine derivatives elucidated here

		CAF-Tyrosol (**6**)	CAF-Ethanolamine (**3**)
Structural formula		$C_{16}H_{18}N_4O_4$	$C_{10}H_{15}N_5O_3$
Molar weight / (g mol^{-1})		330.34	253.27
Crystal system		monoclinic	monoclinic
Space group		$P2_1$	$P2_1/c$
Z		2	4
λ / Å		0.71073	0.71073
Tempoerature / K		296(2)	296(2)
Unit cell dimensions	*a* / Å	10.6394(16)	7.957(3)
	b / Å	5.4724(8)	16.570(6)
	c / Å	13.8989(19)	9.014(4)
	β / degree	110.069(5)	103.050(9)
V / Å^3		760.10(19)	1157.7(8)
Calculated density / (Mg M^{-3})		1.443	1.453
Absorption coefficient / (M m^{-1})		0.106	0.111
θ-range for data collection / degree		1.560-25.052	2.625-25.056
Index ranges		–12 to 12 –6 to 6 –16 to 16	–9 to 9 –19 to 17 –9 to 10
Data collected		6685	7774
Unique reflections		2603	2030
Unique reflections with I > 2σ(I)		1766	1452
Symmetry factor (R_{int})		0.0612	0.0716
Completeness to θmax		99.7	98.8
F (000)		348	536
Parameters refined		217	163
Goodness-of-fit on F^2		0.940	1.161
Final R_1 factor for I > 2σ(I)		0.0592	0.1127
wR2 factor for all data		0.1501	0.3295
Largest diff. peak / hole / (e Å^{-3})		0.432/–0.364	0.486/–0.528
CCDC deposit number		2476994	2476993

a-*c*: unit cell parameters; V: volume; Z: formula unit *per* unit cell; R(int): internal R-value; R1: R-value; wR2: R-value for F2; CCDC: Cambridge Crystallographic Data Centre.

References

1. Agu, P. C.; Afiukwa, C. A.; Orji, O. U.; Ezeh, E. M.; Ofoke, I. H.; Ogbu, C. O.; Ugwuja, E. I.; Aja, P. M.; *Sci. Rep.* **2023**, *13*, 13398. [Crossref]
2. Maia, E. H. B.; Assis, L. C.; de Oliveira, T. A.; da Silva, A. M.; Taranto, A. G.; *Front. Chem.* **2020**, *8*, 343. [Crossref]
3. Pagadala, N. S.; Syed, K.; Tuszynski, J.; *Biophys. Rev.* **2017**, *9*, 91. [Crossref]
4. Silva, L.; Ferreira, E.; Maryam; Espejo-Román, J.; Costa, G.; Cruz, J.; Kimani, N.; Costa, J.; Bittencourt, J.; Cruz, J.; Campos, J.; Santos, C.; *Molecules* **2023**, *28*, 1035. [Crossref]
5. Sheldrick, G. M.; *Acta. Crystallogr. C. Struct. Chem.* **2015**, *71*, 3. [Crossref]
6. Macrae, C. F.; Sovago, I.; Cottrell, S. J.; Galek, P. T. A.; McCabe, P.; Pidcock, E.; Platings, M.; Shields, G. P.; Stevens, J. S.; Towler, M.; Wood, P. A.; *J. Appl. Crystallogr.* **2020**, *53*, 226. [Crossref]

This is an open-access article distributed under the terms of the Creative Commons Attribution Licence.